APPENDIX B.
A Study of the Mechanisms Leading to Re-Ignition in a "Worst Case" Fire Scenario
Final Report, Cooperative Agreement No. 70NANB8H0043

G. Jomaas, B.T. Roberts, J. DuBois and J.L.Torero
Department of Fire Protection Engineering
University of Maryland
College Park, MD20742-3031

ABSTRACT

A systematic evaluation of the stability of a re-circulation zone behind a backward facing step under conditions expected in an aircraft engine nacelle has been conducted together with the evaluation of the effects of the flow structure on a propane diffusion flame established downstream of the step. The objective being to characterize a "worst case" fire scenario. Characterization of the non-reacting re-circulation zone was performed by means of flow visualization. The parameters varied were the flow velocity, step height and surface temperature. Numerical modeling using a Large Eddie Simulation (LES) code has been contrasted with the experimental results. It was observed that for all conditions studied a flow re-circulation zone appears down-stream of the step and is stable but not stationary. The temperature of the floor of the test section was increased up to 600 ^{o}C to explore the effect of buoyancy without the complexity of the reacting flow. Heating of the incoming flow lead to an increase in the dimensions of the re-circulation zone. However, de-stabilization of the flow did not occur. Comparison between the numerical and experimental results shows good qualitative agreement. The caracterization of the flame established behind the backward facing step was followed by a study of the re-ignition potential. The flame was extinguished by separating fuel from oxidizer by means of a plate which was impulsively removed and re-ignition observed. It was established that re-ignition is controlled by cooling and mass transport towards the hot plate. A "worst case scenario" for re-ignition is given by maximizing the fuel mass transfer while keeping the characteristic time for cooling of the fuel surface shorter than the characteristic time to attain a flammable mixture.

1. Introduction

Determination of the efficacy of a suppression agent has been the subject of many studies and an issue of renewed interest after the Montreal Protocol [1]. A general review of the current efforts and literature is provided by Hamins [2]. An area of great concern is that of aircraft where the use of Halon-1301 for fire suppression has been the norm [3]. Different environmentally friendly techniques are under development, among them are solid propellant gas generators.

A gas generator typically consists of a solid propellant tablet, which, upon ignition, rapidly reacts to generate gas phase combustion products and particulate, an igniter to initiate the combustion of the propellant, a filter system, and an exhaust mechanism. This element has been commonly used as a mechanism to inflate air-bags. The principal gas-phase product of the combustion process is nitrogen. Therefore, a logical extension to this technology is fire suppression [3].

If a flame is subject to a fast flow of nitrogen extinction might occur. The advantages of generating this fast flow by means of a solid propellant are many. It is compact, it has a very long storage and service life, it can be used in areas of difficult access, and the response time can be extremely fast. Also, this type of system is considered to have no ozone depletion or global warming potential. One of the main issues that have slowed the development of gas generators as a fire suppression technique is the lack of an adequate test protocol to assess their performance. Estimation of the reliability and efficiency

of this technique depends on a better understanding of the high-speed flow and the fundamental chemical and thermal processes involved in extinction and re-ignition of a fire.

Extinction mechanisms have been a subject of numerous studies and excellent reviews can be found in the literature. A good summary of the existing knowledge is provided by Williams [4]. The process of extinction can be described by means of the Damköhler number (Da=(Residence Time)/(Chemical Time)), by either reducing the residence time or increasing the chemical time a critical Damköhler number for extinction can be attained. The flow originating from burning a solid propellant can reduce the residence time (high velocity flow of products) and increase the chemical time (by directly altering the reactant concentrations, oxygen displacement effect or by decreasing the temperature of the pyrolysis and reaction zones) resulting in sudden extinction of the flame. Furthermore, the interaction between the flame and the flow, coming from the gas generator, can affect the turbulent structure of the system. Local stretch rates can be altered by the nitrogen rich flow resulting in local extinction zones. Depending on the geometry of the system, the type of flame, the characteristics of the gas generator and the distance between the gas generator and the flame the effects of each independent mechanism can be very different. Significant work on the interaction between flames and high speed flow has been reported in the past and have been reviewed by Williams [5] and Blazowski [6] but all the information pertains to scenarios that significantly differ from that of fire flame extinction.

A simple way to increase the residence time is by creating a recirculation zone by means of a backward facing step. This will significantly reduced the strain on the flame and thus provide a “worst case scenario” to test gas generators.

Consider the sudden onset of an enhanced velocity field past a given object. It can be observed that the transient conditions under which the object will continue to burn (or extinguish) differ little from those under which it will continue to burn (or extinguish) in a steady field of equal intensity and distribution. If the flame can not persist after the sudden onset of the velocity it is likely that it will not re-ignite once steady conditions are attained. Cooling down of the fuel will then follow [6]. In the case of solid propellant induced flows the extent and characteristics of the transient and steady state conditions depend on the geometrical configuration. The relative position of the fire with respect to the generator will significantly affect the development and structure of the flow. If the characteristic volume is very large compared to that of the fire and the gas flow induced by the generator, then the transient period will be very short and the flow field will regain its initial characteristics very fast. If the characteristic volume of the flow created by the gas generator is comparable to the volume of the room then a short transient period will be followed by a long steady period (flooding), in this case the flow field will not be expected to regain its initial characteristics. Obstructions in the path between the generator and the fire will significantly affect the velocity and distribution of the flow reaching the fire and will also affect the extent and nature of the transient process.

If flooding occurs it is expected that the critical Damköhler number will be attained permanently and cooling down of the fuel, which is a very slow process (when compared to the chemical and residence times of the flame), will follow. If both transient and steady periods are very short, first scenario depicted above, the flow conditions will provide a Damköhler number that will allow re-ignition if enough gaseous fuel can still be produced when the low velocities and high oxygen concentrations are re-instated [7,8]. Fuel pyrolysis will depend on the surface temperature. When burning, many materials will have a surface temperature much higher than the vaporization temperature (i.e. charring materials). Therefore, fuel pyrolysis will occur even after extinction of the flame. Comparison between the characteristic time of the flow induced by the gas generator and the characteristic cooling time becomes relevant and re-ignition becomes a significant issue when evaluating the performance of gas generators as a suppression mechanisms.

A strong theoretical basis on the areas of ignition and extinction exists but it has never been systematically applied to this type of scenario, therefore, there is a need to evaluate the accuracy of existing theories for a practical situation such as gas generator-fire flame interaction. Addressing all the issues presented is a formidable task that goes far beyond the scope of this study. Suppression is directly linked to the stability and aerodynamic characteristics of the re-circulation zone therefore this work

focuses on the aerodynamic characterization of the flow field behind the backward facing step. A characteristic length scale is defined and used as the main reference parameter. The variables studied are the imposed flow velocity, step height and surface temperature. Reacting flow experiments are conducted and correlated with the different flow conditions to describe the effect that the flow will have on the structure of the flame. Conditions leading to re-ignition are explored as a further parameter that will serve to characterize a "worst case" fire scenario.

2. Experimental Facility

The experimental set-up consists of a wind tunnel and a test section. The dimensions and characteristics of the wind tunnel are defined to guarantee a fully developed flow field, at the entrance to the test section, for all the experimental conditions studied. The test section incorporates a variable height step that can be varied from a step to duct ratio (H/D) of approximately 0.05 to 0.6. Figure 1, below, depicts a global view of the experimental setup where each component of the setup is labeled.

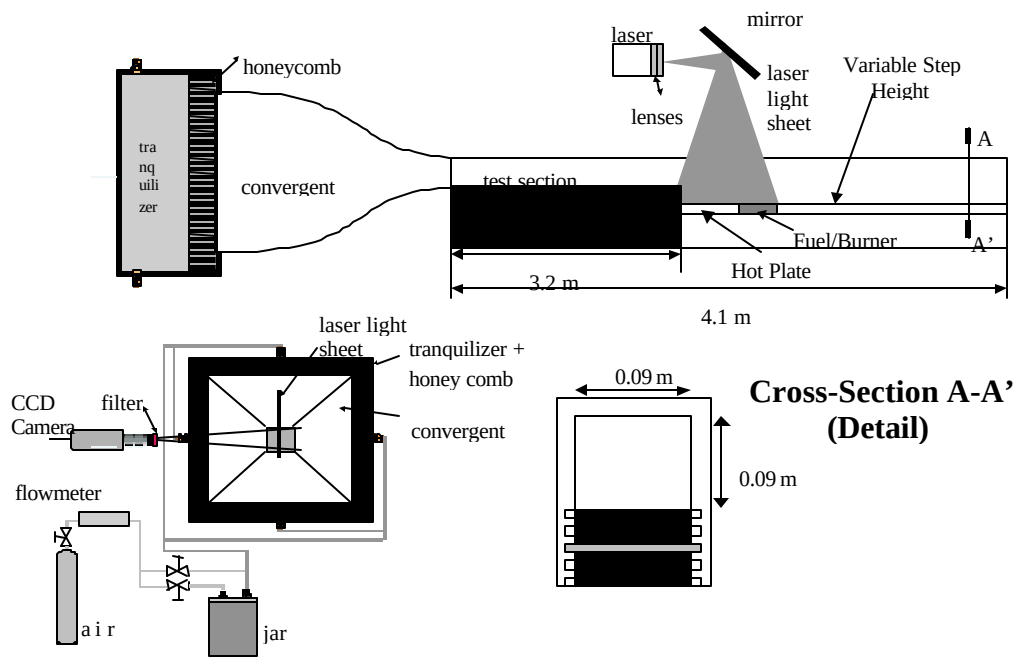

Figure 1 Schematic of the Experimental Apparatus

Air is fed from the compressor to the particle-seeding canister and then to the convergent. A valve from the compressor to the canister allows the mass flow of air to be controlled. From the valve the air flows through a pipe to a tube of diameter 12.7 mm which feeds into the canister. From the canister is another tube, which feeds into the convergent.

The convergent has an 8:1 ratio with a square inlet of dimension 0.72 m by 0.72 m by 0.30 m. A 50 mm thick honeycomb sheet is placed across the entire cross section to help disperse the flow and make it uniform. The convergent leads to a duct of cross section of 90 mm by 90 mm. The duct is 3.2 m long to allow the flow to become fully developed at the outlet.

The test section is attached to the outlet of the wind tunnel. The floor of the test section consists of a stainless steel sheet with dimension 0.090 m by 0.90 m. At the end closest to the wind tunnel outlet, pieces of the sheet can be removed. This creates room for the hot plate and the burner. Also, the step

height can be adjusted from being level to the bottom of the wind tunnel outlet to being 100 mm below the bottom of the wind tunnel outlet. The test section is made of an aluminum frame with glass sides and a glass top. The Robax glass used has a normal operating temperature up to 700°C for long-term usage and an extreme operating temperature of 800°C for short-term usage. It is highly transparent, which allows the laser beam to illuminate particles within the test section and the camera to view the images.

A hot plate is used to characterize the effects of buoyancy on the recirculation zone. The top layer of the hot plate is a sheet of copper. This 1 mm thick sheet fits exactly into the hole left by the removable piece from the stainless steel bottom sheet. Copper is used because of its high thermal conductivity leading to a homogeneous distribution of temperature across its entire surface. Three thermocouples are spaced evenly across the length of the copper plate, and a sheet of stainless steel is placed below them. The stainless steel sheet is resting on a thin layer of cement. Kanthal wire with a diameter of 0.25 mm is coiled evenly covering most of the surface area underneath the cement. An AC voltage source is attached to the ends of the Kanthal wire. The copper plate can reach temperatures up to 600 °C. A 20 mm thick insulation covering is placed below the wire. Total heat flux from the plate to the flow can be evaluated following the methodology presented in references [8,9].

The burner has a fuel inlet at the bottom. A 10 mm thick plate of sintered bronze is placed above the fuel inlet, and serves as a flow rectifier. Glass beads are placed over the bronze filling the inside of the burner. Finally, a lid made of 10 mm thick sintered bronze is placed on top. The lid is held in place with a high temperature gasket sealant. Two different fuels are used for these experiments, gaseous propane and liquid n-heptane. The same burner is used for both fuels.

A red Laser diode with maximum output of 0.5 watts provides a 60 mm by 1 mm thick light sheet. The light sheet is positioned such that the width is parallel to the flow direction of air. The sheet is, for most experiments, positioned at the center of the test section but it can be displaced towards the walls to observe three-dimensional structures.

A monochrome digital camera model 4910 from COHU, Inc. is used to capture the images. The camera resolution is 580 x 350. The electronic shutter is designed for an exposure of 1/60 seconds. A zoom lens with a narrow band filter is attached to the aperture of the digital camera. The zoom lens is attached to achieve a magnification of up to 10 times. For smoke visualization, the zoom lens is adjusted to observe the entire portion of the test section illuminated by the laser beam. Two different video cards are needed to operate the video processing camera and software properly. These cards are a Matrox Graphics Architecture video card and a PIXCI imaging board.

3. Experimental Results

Experiments have been conducted to characterize the re-circulation zone and establish a window of stability. Further experiments will use this window of stability to study the heat transfer mechanisms and the re-ignition process. Experiments have been conducted with step heights less than 55 mm and flow velocities ranging from (0.5 to 5.0) m/s. The flow temperature has been varied between 25 ºC and 600 ºC by means of the previously described hot plate.

3.1. Flow Visualization Methodology

Flow visualization was conducted by seeding the principal flow and illuminating the particles with a laser sheet. It was initially observed that the re-circulation zone pulsated at a well-established frequency that varied between (3 to 8) Hz, depending on the flow velocity. Entrainment of the seeded particles into the re-circulation zone was found to be weak. Fluctuations together with particle entrainment made visualization difficult. A number of traditional means of visualization were attempted (smoke generation, talc powder, etc.) with no success.

Kanthal wire was placed at the step and 3 mm above the surface. Beads of solder oil were distributed on the wire. Then the wire was heated electrically generating a smoke trace following the streamline closest to the surface. Clearly, the distance between the wire and the surface will represent a

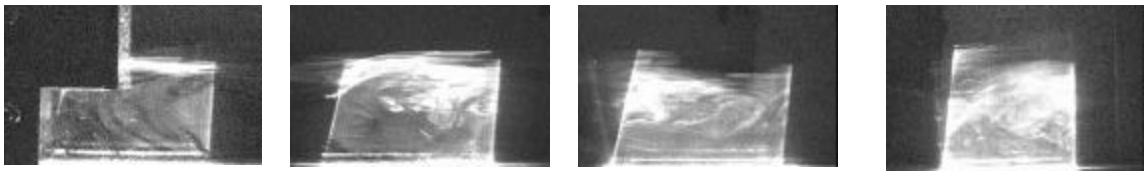

Figure 2 - Sequence of smoke visualization images

minimum error inherent to this methodology. The region of interest was divided into 60 mm sub-sections, and as shown in Figure 2, the smoke traces was detected by means of the CCD camera. Fluctuations of the flow made an averaging process necessary, and the method used is described below.

A sequence of 25 images was captured by means of the EPIX XCAP Software. The images were treated independently, and each one was digitized to a gray level. The sequence was then averaged, and an assigned binary threshold value provided a black and white picture indicating the path of the smoke. The threshold had to be defined carefully since smoke traces changed with increasing distance from the step. At the beginning of the test section the smoke was concentrated in a narrow area (Figure 2), so a high threshold value was needed to obtain adequate contrast. Towards the end of the re-circulation zone the smoke was more dispersed, and a lower limit was needed to obtain a clear picture of the smoke. All sections were assigned several threshold values in the critical regions, and consequently, discrepancies in the manipulation process of the pictures were minimized.

By identifying the locus of the maximum intensity the borderline of the averaged re-circulation zone can be determined, and thus the averaged re-circulation zone length, X_r.

The averaged gray area can be further binarized to obtain the average amplitude of the fluctuations. Figure 3 shows the composition of a sequence of averaged images corresponding to the individual pictures of Figure 2. As can be observed, the flow fluctuates in the horizontal and vertical direction. The length and height of the re-circulation zone can be complemented by the amplitude of the fluctuation (ΔH_r, ΔX_r).

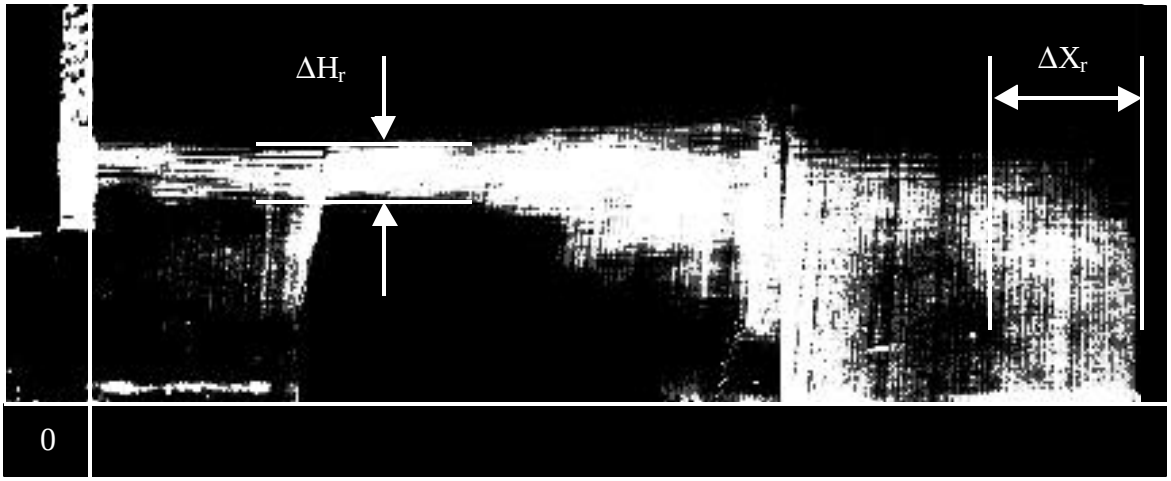

Figure 3 – Sequence of averaged images showing the extent of the re-circulation zone and corresponding to an airflow velocity of 1 m/s with a step height of 57 mm.

3.2. Flow-Visualization Experimental Results

Individual observation of each image obtained in a sequence showed that the re-circulation zone was stable but not stationary for all condition studied. The length and height of the re-circulation zone varied in a periodic fashion. The amplitude of the fluctuations was always less than 20 % of the characteristic length. This can be observed for the particular case presented in Figure 3. The frequency of the fluctuations varied from (3 to 8) Hz and depended on the flow velocity and the step-height. The flow was observed to re-attach after the re-circulation zone without noticeable periodic vortex shedding.

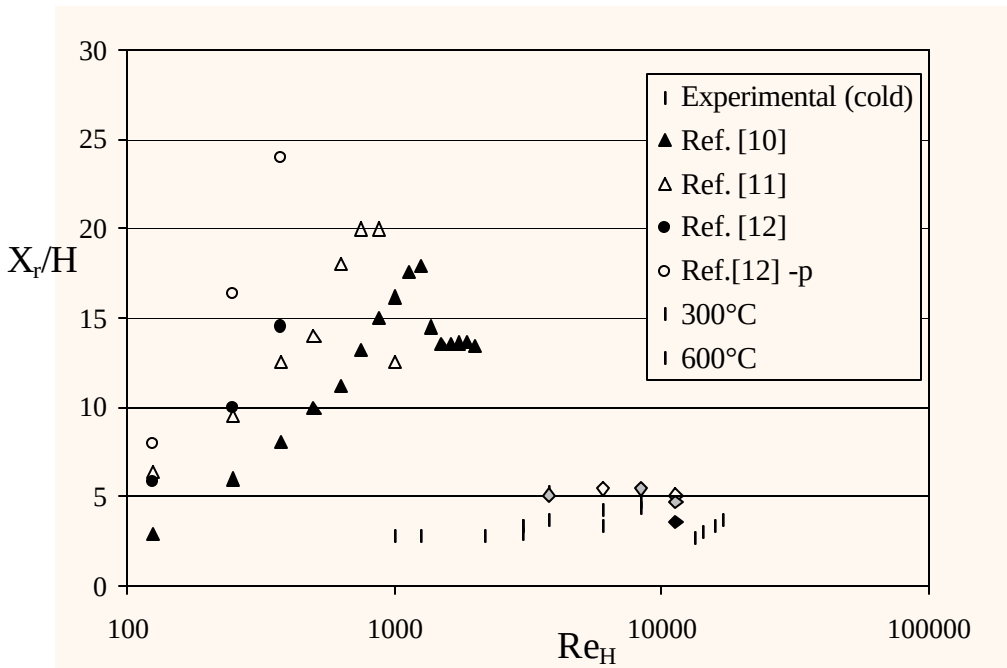

Figure 4 – Evolution of X_r/H as a function of Re_H.

Analysis of the average re-circulation zone showed a weak increase with the Reynold's number as shown in Figure 4. The values are normalized by the step height. Only representative values are presented to avoid overcrowding of the figure. The normalized characteristic length scale increases with Re_H until it reaches a maximum value. A further increase in Re_H leads to a decrease in the re-circulation zone length towards an almost constant value. Although the trends are similar to those previously reported in the literature [10-13], the characteristic length of the re-circulation zone is observed to be much smaller. This is not a surprising observation, since the geometry and characteristic flow velocities typical of this study are much smaller than those used in the references listed.

An increase in the surface temperature results in a larger re-circulation zone (both H_r and X_r) but the stability seems unaffected by the temperature increase. Data is presented for three temperatures: 25°C (ambient), 300 ^{o}C, and 600 ^{o}C. It can be observed that the surface temperature has a minor effect on the length of the re-circulation zone. Higher temperatures could not be attained due to melting of the Kanthal wire used in the heater.

3.3. Reacting Flow Experiments

Figure 5 shows the different regimes of the flame as a function of both propane flow rate and flow velocity. The images correspond to a step height set at 57 mm but can be generalized to other step heights. For low forced flow velocities and fuel injection the flame established in the re-circulation area is blue and seems to spin with the flow (Regime 1, Figure 5(a)). Increasing the fuel injection velocity or

the forced flow velocity increases the size of the flame and begins to show a yellow glow characteristic of diffusion flames (Regime 2, Figure 5(b)). The flame remains attached to the burner but as the forced flow and fuel injection velocities increase the flame is deflected towards the step (against the flow) indicating the dominant role of the recirculating flow (Figure 5 (c)). When this regime is fully established, the flame becomes attached to the edge of the step and it begins to detach from the burner surface. The entrainment velocity seems to have reached the blow-off limit at the trailing edge of the burner. Regime 3 corresponds to a flame attached to the edge of the step, but totally established at the interface of the main flow and the re-circulation zone. The flame is no longer attached to the burner (Figure 5(d)). The flame is yellow and characteristic of a diffusion flame.

Figure 6 shows the experimental conditions that delimit the three different regimes. An increase in the step height will result in attainment of Regime earlier. The border curves are displaced towards the origin. The burner is placed 100 mm downstream of the step. When the burner was placed closer the regimes were the same but transition towards the final condition was faster. Observation of the streamlines obtained from the smoke visualization showed that air entrainment occurred mostly at the downstream edge of the recirculation zone (Figure 3) therefore Regime 1 was enlarged by placing the burner in this region. It is important to note that the flame seems to displace towards the interface due to lack of oxidizer inside the re-circulation zone. Thus, entrainment seems to be the controlling mechanism behind the flame geometry.

Regime 2 corresponds to what Takahashi et al. [14] label Regime I, the flow limitations of the present configuration did not allow to migrate to their Regime II where enhanced oxidizer supply to the recirculation zone results in a wake stabilized flame. Takahashi et al. [14] do not report the presence of Regime 1 as observed in the present work.

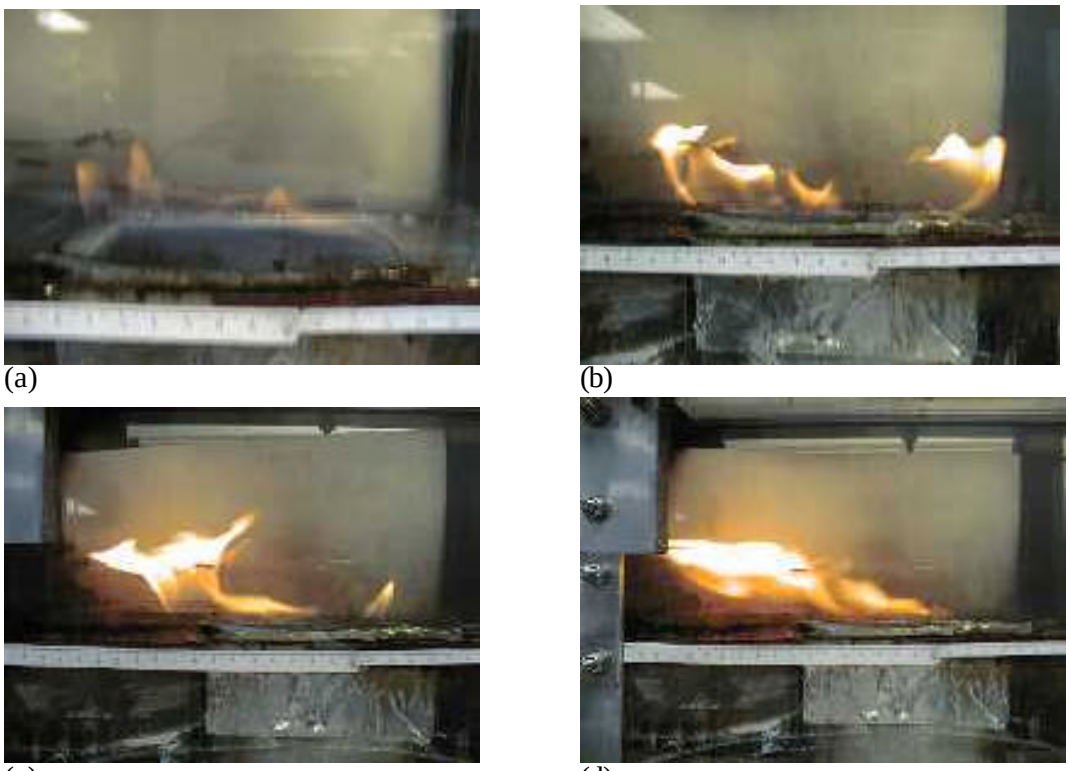

Figure 5 Sequence of images corresponding to the three different flame regimes observed.

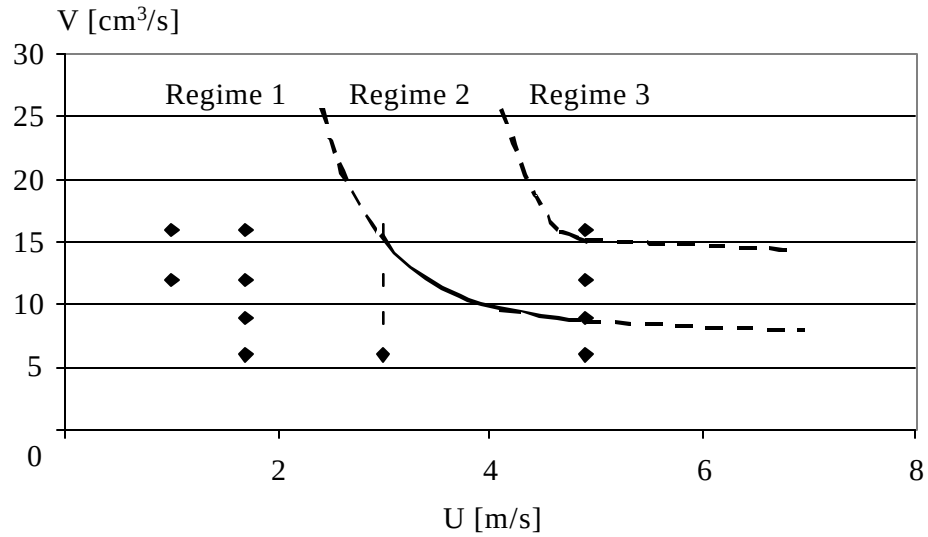

Figure 6 Different regimes of the flame, all tests presented were performed for a 57 mm step height.

3.4 Re-Ignition Experiments

3.4.1 Methodology

The experiments done with smoke and propane indicated that air entrainment towards the re-circulation zone controls the stability and characteristics of the flame therefore, after suppression, re-ignition can only occur upstream of the burner. Fuel and oxidizer will only be present in this region. The hot plate was therefore placed directly adjacent to the step, followed by the burner. This defined the "worst case" scenario for re-ignition. The length of the hot plate was defined based on the characteristic length of the re-circulation zone (X_r). Liquid n-heptane was used as fuel substitute even though jet fuel would have been a more relevant fuel. The quantitative results, thus, only correspond to n-heptane but the general observations can be generalized to other more relevant fuels. Jet fuel was avoided because of the large soot production characteristic of this fuel, which made visualization difficult. Again, experiments were conducted for different step heights, temperatures, and flow velocities. The n-heptane was delivered continuously by the means of a simple gravity tank that guaranteed a constant fuel level at the burner surface.

The experimental procedure was kept consistent for all tests. First the hot plate was heated until a constant temperature was achieved. Once the hot plate temperature varied less than 5 ^{o}C/min, supply of fuel and oxidizer was initiated together with data acquisition. At this point the flame was ignited. Finally, the fuel amount and the hot plate temperature were adjusted to be within the desired range.

The porous plate allows heat and fuel transfer to the interior enabling a slight variation of the fuel supply. This was evidenced in larger or smaller flames depending on the position of the gravity tank. The position of the gravity tank was varied within the possible range to allow for a study of the sensitivity of the present observations to the fuel supply.

The presence of the flame generated variations in the hot plate temperature therefore it was necessary to vary the current supply to the Kanthal wire and to wait until steady conditions were resumed.

The data collected during the experiments were temperature, re-ignition delay time, flow velocity, and step height. The temperature was measured with thermocouples placed at three different nodes along the length of the hot plate, where the one furthest from the step was located exactly between the hot plate and the burner frame. Time measurements were taken manually, and due to the uncertainty in the human reaction, recorded in integer values of seconds. The experiments were always run in whole sequences

ranging from 0.5-5.0 m/s at a temperature as consistent as possible. Thus, when something interfered during a sequence, a new sequence was started from scratch.

The auto-ignition temperature of n-heptane ($CH_3(CH_2)_5CH_3$) is 247.2ºC [15]. Therefore, a temperature at the hot plate around 400ºC was taken as a starting estimate for where re-ignition could occur. The location of the re-ignition point was established setting the origin at the step and with the positive direction following the principal flow direction.

3.4.2. Extinction Protocol

When the flow, the temperature, and the step-height were as specified for the test, the flame was extinguished by sliding a sheet of stainless steel over the burner. This separated fuel and oxygen, and consequently the flame could not sustain. The sheet was removed quickly immediately following visual observation of extinction. The time was recorded from the moment the plate was removed. Sometimes re-ignition occurred immediately, that is, as soon as the sheet was removed, indicating no re-ignition delay time. However, most of the time, there was a delay before re-ignition occurred. For certain combinations of fuel, flow velocity, and temperature the re-ignition delay time approached infinity. Details of these conditions will be presented later.

Here, re-ignition delays longer than forty seconds are considered to approach infinity. This time is significantly longer than any of the reported ignition delay times [16,17].

3.4.3. The Origin of Re-Ignition

To determine the locus of the re-ignition test sequences were videotaped and the re-ignition process was observed frame by frame. The images showed that re-ignition occurred always in the gas above the hot plate. Infra red-imaging of the test section showed no particular hot spots in any of the surfaces so local re-ignition was not considered. By comparing the infra-red data, it could be concluded that the temperature over the hot plate was (10 to 15) % higher than the temperature elsewhere.

3.4.4. Re-Ignition Results

For re-ignition to occur in this particular scenario, several different processes are necessary. The combustible surface needs to remain hot enough to continue producing gaseous fuel. The fuel vapor has to mix with the hot oxidizer gas and form a combustible mixture near the surface of the hot plate and the hot plate has to transfer sufficient heat to lead to initiation of a gas phase combustion reaction. Cooling down of the fuel surface, heat transfer from the hot plate and residence time of the fuel mixture inside the re-circulation zone are all controlled by the flow. The different experimental observations will be described in an attempt to isolate the controlling parameters of the re-ignition process to establish a worst case scenario.

The first experiments were done at a step height of 57 mm, this step height was chosen because it provided a stable re-circulation zone and flame for a broad range of flow conditions. At this height the flame is bright yellow for all flow velocities. For velocities lower than 2.5 m/s the flame flickers down the length of the tunnel, whereas the flame attaches to the tip of the step for higher velocities. Figure 7 shows the flame development as a function of velocity. This indicates a more significant mixing of fuel and oxidizer over the hot plate for the higher flow velocities.

The re-ignition delay times were fairly consistent for a step height of 57 mm, and with few discrepancies, all times were below 3 s. Table 1 contains sample data for a step height of 57 mm. Table 1 shows that the re-ignition delay increases for the low (u_∞ < 3 m/s) and high flow velocities (u_∞ >5 m/s). This pattern is consistent under different experimental conditions. As and example, Figure 8 shows the re-ignition delay time as a function of velocity at five different temperatures. It can be seen that although the above mentioned pattern remains constant the hot plate temperature does not have a consistent effect

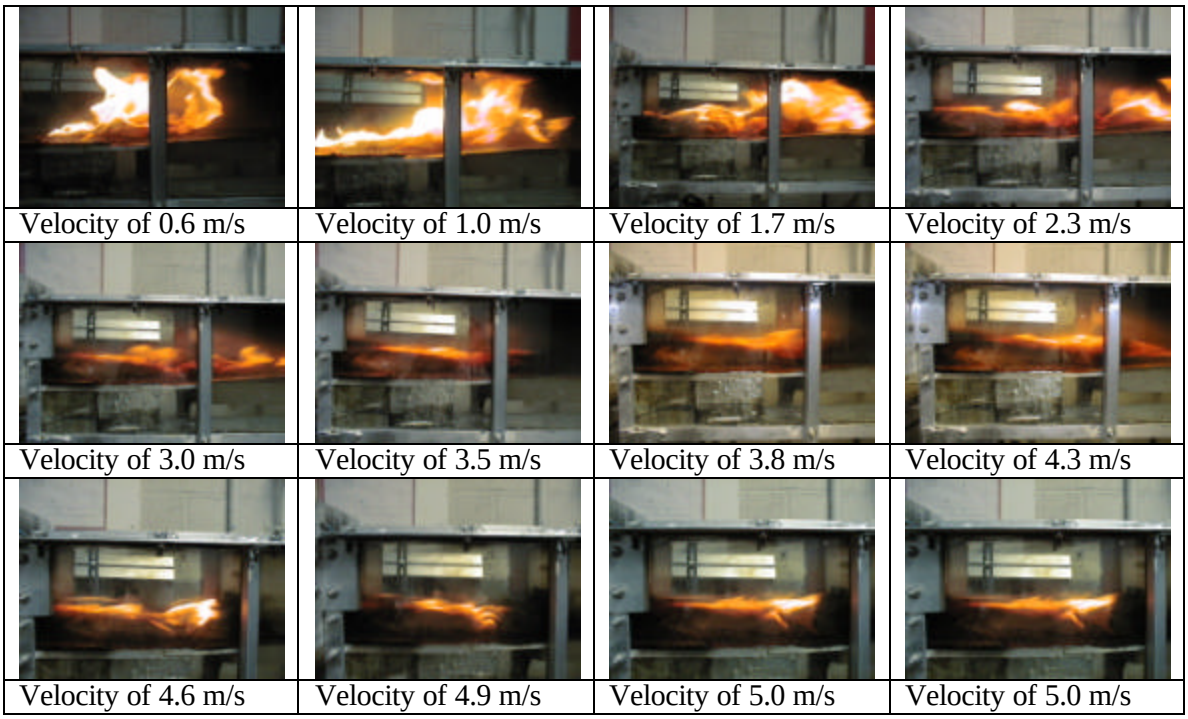

Figure 7 Flame development as a function of velocity for n-heptane

AIR FLOW VELOCITY [M/S]	TEMPERATURE [ºC]	IGNITION DELAY TIME [S]
0.6	349	3
1	351	3
1.7	353	2
2.3	353	2
3	354	2
3.5	352	1
3.8	351	1
4.3	350	0
4.6	347	0.5
4.9	347	1
5	345	0
5	344	1.5
5	342	0
5	340	1.5

Table 1 Data sample for step height of 57 mm

on the ignition delay time. The differences seem to be within the experimental error, therefore an average for all different temperatures was taken and is presented in Figure 9.

These results suggest two primary, and competing, mechanisms that control the re-ignition process, convection and induction. The phenomenological explanation that will be provided here is consistent with arguments previously used when addressing ignition of condensed fuels [16,17].

The effect of convection is complex since in this particular case an increase in the flow velocity will result in an increase in the characteristic velocity within the re-circulation zone but will also increase the length of this region. Thus, variations in the characteristic velocity within the re-circulation zone will result in changes in the amount of fuel carried towards the hot plate at the fuel surface. An increase in the velocity will increase cooling at the fuel surface and also mass transfer. In contrast, the induction time can be described in easier terms therefore will be addressed first.

If the ignition temperature of the flammable mixture is assumed to be constant the induction time will only depend on the rate of heat transfer at the hot plate surface. So, if the hot plate has a finite length and constant temperature, a change in velocity will result in a decrease of the time available for the combustible mixture to attain the ignition temperature. The convective heat transfer coefficient being a function of $Re^{1/2}$ and the residence time an inverse function of the characteristic velocity. This effect was made obvious by re-ignition occurring closer and closer to the backward facing step as the velocity increased. The characteristic time available over the hot plate is of the order of a 0.1 s and thus falls within the experimental error, so proper quantification of this effect is not possible. Therefore, the main requirement for the hot plate has to be at a high enough temperature to deliver sufficient heat to the gas mixture faster than the characteristic residence time. In summary, if the induction time (time to for the flammable mixture to attain a temperature were heat losses are smaller than the heat generated by the chemical reaction) is smaller than the residence time (time that the flammable mixture remains over the hot plate) then re-ignition will occur. Definition of an appropriate Damkhöller number is therefore possible.

The above observations explain why the hot plate temperature needs to be much higher than the auto-ignition temperature of the fuel. The auto-ignition temperature of n-heptane is 247.2 ºC [15] and as presented in Table 1 the re-ignition temperatures are always above 340 ^{o}C. Furthermore, this explains why the re-ignition delay times are not sensitive to the hot plate temperature.

The specific geometry used is responsible for the re-ignition temperature, therefore it is of great importance to note that, for the present configuration, an increase in the plate length should result in a decrease in the re-ignition temperatures only if the flammable mixture supplied from the burner remains constant. Since the flammable mixture is determined by the effects of the re-circulation zone on the burner (as will be detailed later) and this is linked to the flow conditions, and increase in the burner length will not necessarily speed re-ignition. The results presented above correspond to what was found to be the "worst case scenario" and were chosen for presentation because they provided the broadest range of re-ignition conditions.

The above observations justify neglecting the induction time and averaging the data for different hot plate temperatures, as presented in Figure 9. Is in this context that the effect of convection on the fuel surface will be analyzed.

Fuel supply towards the hot plate is controlled by two competing mechanisms, mass transfer and heat transfer at the fuel surface. For low flow velocities the fuel concentration reaches the lean flammability limit before cooling of the fuel surface has been reached, for high flow velocities the fuel surface cools down before the lean flammability limit has been attained.

For $u_\infty < 4$ m/s, mass transfer from the fuel surface to the gas flow controls the re-ignition delay time. Mass transfer is also a function of $Re^{1/2}$ therefore increases with the flow velocity. When the plate covers the fuel the re-circulation zone is filled with air and the fuel is washed away. So when the plate is removed fuel starts migrating towards the hot plate but it will not ignite until the gas phase mixture attains the lean flammability limit. If the induction time can be neglected ignition will occur at this point. Transport of fuel is proportional to the flow velocity therefore the re-ignition time will decrease as the flow velocity increases.

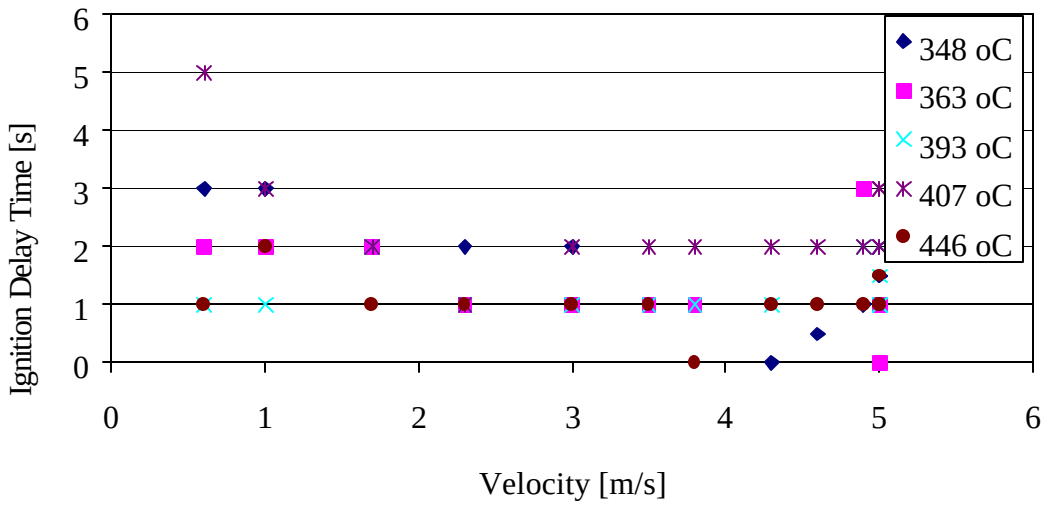

Figure 8 Ignition Delay Time as a Function of Velocity at Different Temperatures for a step height of 57 mm.

For $u_\infty > 4$ m/s, cooling of the fuel surface is the controlling mechanism. Convective heat transfer is also proportional to $Re^{1/2}$ therefore cooling of the fuel surface will be enhanced as the flow velocity increases. The fuel vaporization rate can be considered to follow an Arrhenius law therefore the decrease of the fuel mass flux can be expected to be more abrupt as the surface temperature decreases. The re-ignition delay time is expected to increase abruptly as the velocity increases. A threshold will be attained beyond which the fuel will cool before the lean flammability limit can be attained. The averaged data presented in Figure 9 serves to validate this phenomenological explanation. As observed in Figure 9, re-ignition can not be accomplished for $u_\infty > 5$ m/s.

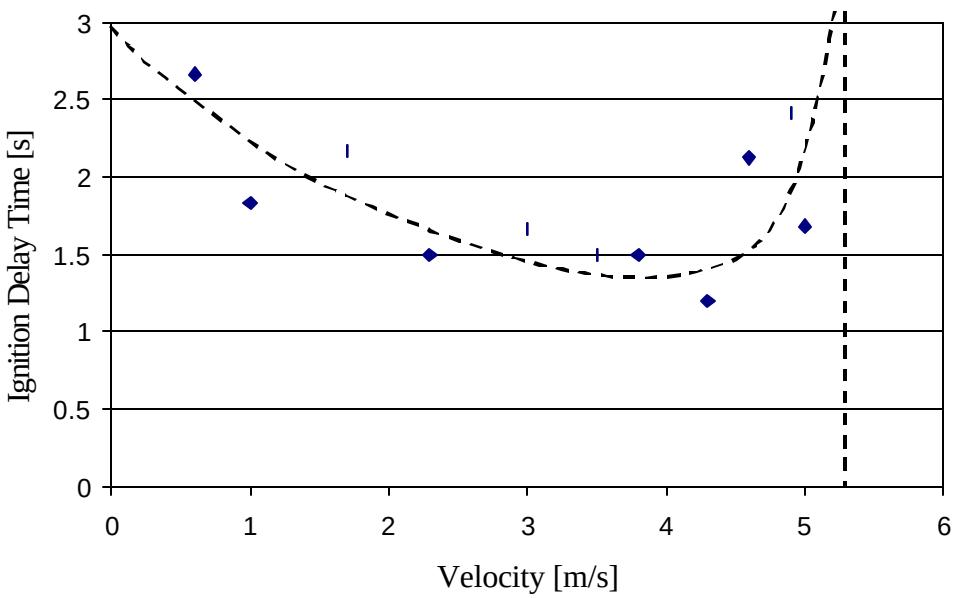

Figure 9 Average Ignition Delay Time as a Function of Velocity

The 57 mm step height corresponded to the shortest re-ignition delay times. If the step height decreases the re-ignition delay times increase significantly because the re-circulation zone ends before the trailing edge of the burner, therefore it requires more time to achieve a flammable mixture. The results at a step height of 32 mm are presented in Figure 10. At flow velocities higher than 4 m/s, the ignition delay time approached infinity (as defined previously) for all temperatures. This maximum flow velocity is lower than that for 57 mm indicating again a minimum evaporation rate necessary to attain a flammable mixture before cooling of the fuel surface dominates. A decrease in the area contributing fuel results in a decrease in the total amount of fuel inside the re-circulation zone, therefore a higher evaporation rate is necessary. At 19 mm, the lowest step height tested, the ignition delay time approached infinity for all flow velocities and all temperatures (as high as 530ºC) tested. Similar results can be obtained for larger step heights where the re-circulation zone ends down-stream of the trailing edge of the burner, thus entrains significant amount of excess air before the fuel enter the re-circulation zone.

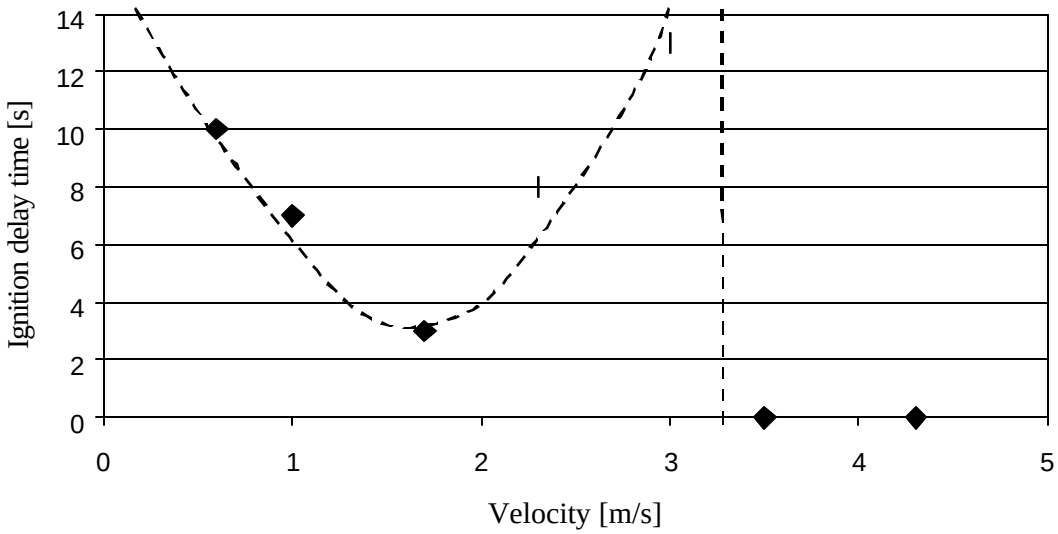

Figure 10 Ignition delay time as a function of flow velocity for a step height of 32 mm, and a temperature of 440 °C

4. Numerical Modeling

The code LES-3D [18] has been implemented on both a Pentium II PC Computer and a DEC-Alpha workstation. Tecplot and Smoke-View provide a visual interface for LES-3D. The code has been used to model the experimental conditions described above. Emphasis has been given to the study of the cold flow. Only a brief summary of this work can be found in reference [19].

Work has focused on using large eddy simulation to model the dynamics taking place in the wind tunnel. Initial work with the code utilized a control volume approach to look at velocity. The boundaries of the computational field were defined as a constant cross section rectangular prism having the dimensions of the actual test section portion of the apparatus. The dimensions of the prism were 0.090 m wide, 0.90 m long and 0.15 m high. The air flowed along the length of the prism. Mass entered normal to the inlet cross sectional area through an 0.090 m by 0.090 m vent extending downward from the top of the prism, and exited through a 0.090 m by (0.090 + H) m vent, where "H" is the step height.

4.1. Preliminary Validation

Prior to running simulations through a mock-up of the test section, a straight 0.90 m duct was modeled with the cross sectional dimensions of the inlet. Specifying a fully developed velocity profile, initial simulations were executed to determine whether both non-slip boundary conditions were preserved, and y- and z- velocities vanished across the domain for a 1.0 m/s flow travelling the length of the duct. This did hold true. Centerline velocities decayed as predicted terminating at the walls. Profiles generated from velocity sampling routines indicated that the flow was symmetric about the y- and z- axes. Likewise, speeds decayed as expected as they traveled down the duct.

4.2 Entry Profile

To generate a computerized flow scenario that could be compared to that moving through the actual apparatus, a means of representing the velocity profile in the coding was necessary. This was done by varying slip conditions, alternating between pre-set velocity profiles (top hat or parabolic), and changing the length of the inlet into the test section. The hope was to generate inlet conditions at the test section entrance that matched the flow through the actual apparatus and accurately predicted the size of the re-circulation zone. An inlet section was added into the computational field by constructing an obstacle a few centimeters into the rectangular prism representing the test section. The test section itself was extended such that the length of the duct after the step remained 0.90 m in length. It was discovered that changes in these parameters significantly changed the length of the average re-circulation zone (X_r). The end of the average re-circulation zone is defined as the location of a zero horizontal velocity vector. A list of the different Test cases is presented in Table 2.

Table 2 shows quantitative differences on the average re-circulation zone length between the different initial conditions studied. The average re-circulation zone length is influenced by the nature of the incoming flow. Allowing the flow to develop (x=-0.25 m and x=-0.90 m) results in a change in the size of the average re-circulation zone that is not a direct function of the developing distance. It was found that beyond x=-0.90 m the average re-circulation zone attained a constant length. The boundary condition (slip, partial-slip, and non-slip) affected the development of the flow, and consequently X_r. A non-slip boundary condition resulted in a shorter developing distance, thus was preferred. Imposing a parabolic profile or specified volume condition at the inlet also had a significant effect on X_r, in both cases the developing distance was much larger than for the Top-Hat profile.

Velocity measurements were compared with the predictions of the LES-3D code for a Top-Hat profile placed at x=-0.90 m. The results are presented in Figure 11. As it can be observed, the velocity

Velocity Profile	**Slip condition**	**Inlet Length**	**X_r**	**U supplied**	**Centerline Inlet Velocity**	**Average Exit Velocity**
Top Hat	Partial	0.00 m	0.40 m	1.0 m/s	1.00 m/s	0.6 m/s
Top Hat	partial	-0.25 m	0.45 m	1.0 m/s	1.08 m/s	0.7 m/s
Top Hat	partial	-0.90 m	0.43 m	1.0 m/s	1.13 m/s	0.7 m/s
Top Hat	Non-slip	-0.90 m	0.41 m	1.0 m/s	1.30 m/s	0.7 m/s
Parabolic	Partial	0.00 m	0.40 m	1.5 m/s	1.50 m/s	0.3 m/s
Parabolic	Partial	-0.25 m	0.32 m	1.5 m/s	1.30 m/s	0.5 m/s
Parabolic	Non-slip	-0.90 m	0.37 m	1.5 m/s	1.32 m/s	0.5 m/s
Vol. Flux specified	Non-slip	-0.90 m	0.46 m	1.0 m/s	1.08 m/s	0.7 m/s

Table 2 Test cases for a specific characteristic inlet velocity of 1.0 m/s and 1.5 m/s.

profile predicted by the LES-3D code corresponds better to that measured for a laminar flow (0.8 m/s), the flattening of the profile, characteristic of initiation of turbulence is not well captured. Vector profiles of the flow were produced in the straight duct study. Top hat flows were found to develop turbulent profiles after travelling 0.40 m. The boundary layer thickness of the profile, however, was slightly greater than what one usually observes for turbulent flows. The speed remained constant by the time it had traveled 0.90 m, a distance equivalent to the entire length of the test section for both the partial and non-slip scenarios.

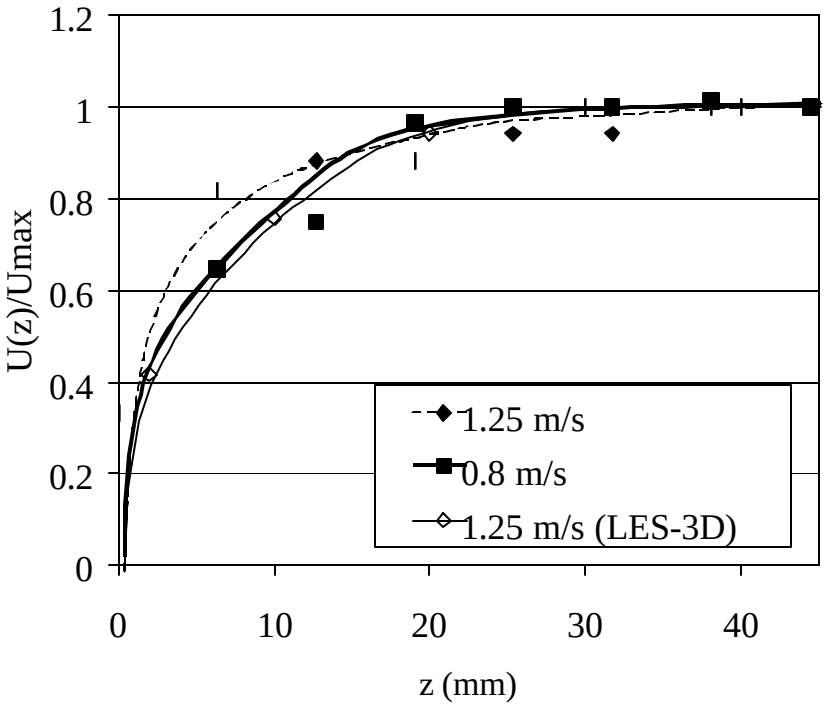

Figure 11 Comparison of normalized velocity profiles

For the particular conditions presented here the experimental re-circulation zone was 0.29 m, as measured with particle laser imaging in the wind tunnel with the same inlet flow speed. Some of the discrepancy in the length of X_r measured in Tecplot could be attributed to averaging of pulsing re-circulating fluid particles behind the step.

As a result, we chose to simulate the problem with the LES-3D/IFS code as a top hat flow through a 1.80 m rectangular prism with non-slip surfaces that featured a 0.90 m obstacle to represent the duct inlet. Consequently, flows were permitted to develop fully and naturally prior to entering the test section. The LES-3D permits the user to specify a velocity profile. Nonetheless, defining an exact equation U (x) for the entire domain of the rectangular closed surface would be an arduous task of questionable value, given the gross nature of the physically measured profile at the walls. Typical profiles for turbulent flows such as $u_{avg.} \propto (y/\delta)^{1/7}$ [10] fail to give reasonable approximations of experimental results near the wall. Running the 1 m/s top hat non-slip flow through the step model yielded a 0.41 m re-circulation zone.

4.3 Re-circulation Zone length (X_r)

The variation in the re-circulation zone length and stability was determined and is presented in Figure 12. All the different step heights assigned were less than 55 mm high. The numerical predictions

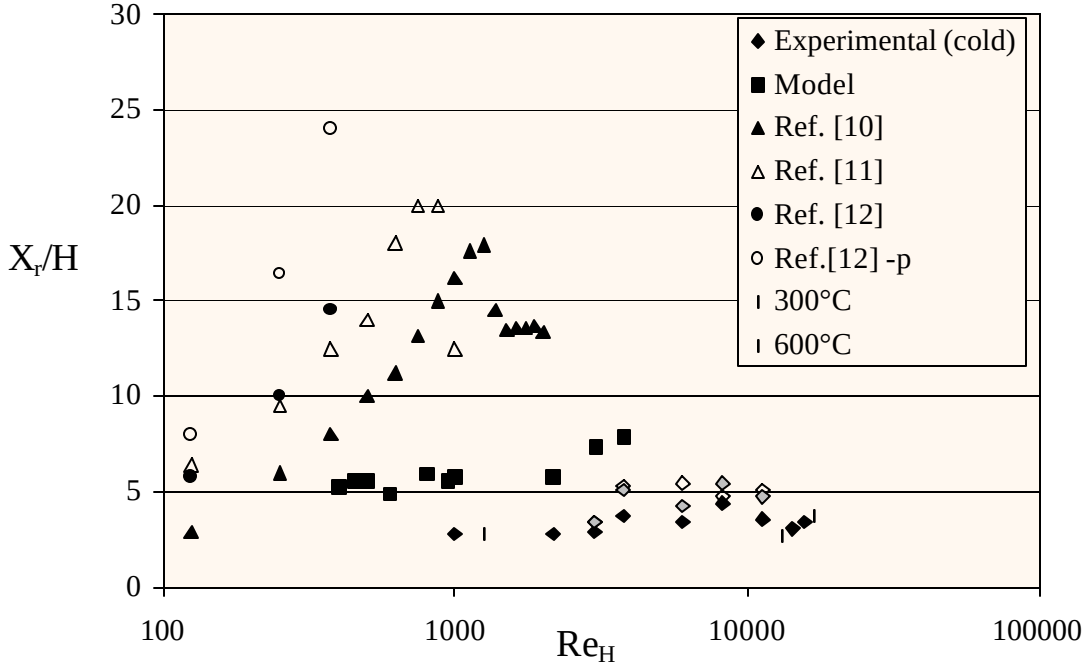

Figure 12 Normalized re-circulation zone length scale as a function of Re_H.

underestimate the data from the literature but the trends correspond well to those observed experimentally.

The experiments available in the literature were conducted under conditions very different from those of the present experiments. In general, velocities were much higher and the aspect ratio significantly larger. The average re-circulation zone does not provide any evaluation of the stability of the re-circulation zone. Therefore, an analysis of the time dependent velocity was conducted to identify vortex shedding.

Velocity measurements were made 76 mm apart down the centerline of the simulated test section at four different heights: test section floor (0 mm), mid-step height (28.6 mm), step height (57.2 mm), and mid inlet (102.1 mm). Time dependent velocity measurements are presented in Figures 13 and 14 for two different positions along the duct. Figure 13 shows the velocity evolution at the inlet. A cross section at a distance smaller than X_r is shown on Figure 14. Strong fluctuations of the velocity around the mean value can be observed. The velocity measurements inside the re-circulation zone are characterized by negative values and by a mean value much smaller than the main flow. Beyond the re-circulation zone (Figure 14) the fluctuations decrease in magnitude and there is a total absence of negative velocities. The absence of negative values and the homogeneity of the flow seem to imply an absence of vortex shedding.

It was assumed that the re-circulation zone would be demarcated by the position where one duct-floor measurement resulted in a negative velocity and its downstream neighbor measured a positive velocity. Pulsing therefore should be traceable by watching where this negative-to-positive phenomenon occurs and noting whether it sweeps back and forth across the computational domain. The LES-3D code was set to take instantaneous measurement of velocity along the duct floor and produce a data file of the speeds recorded as a function of time. It was determined that X_r/H varies from 4 to 12 with a mean value of approximately 6, with these being independent of the Reynolds number. Although larger than the fluctuations observed experimentally these perturbations seem to follow similar trends.

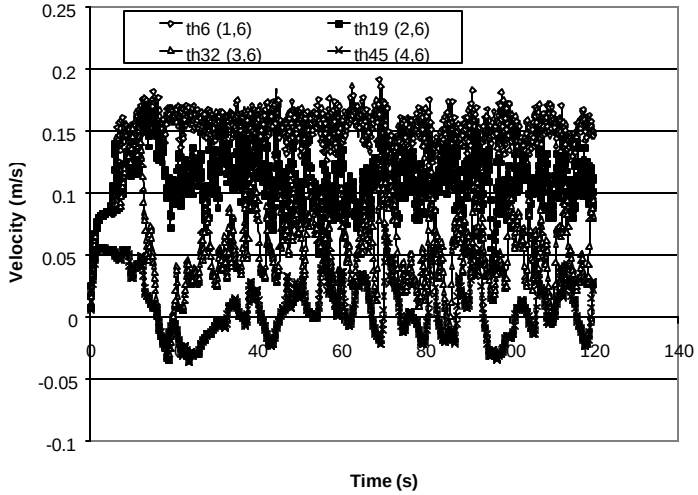

Figure 13 – Time evolution of the velocity for Re=600 measured at x=0.381 m

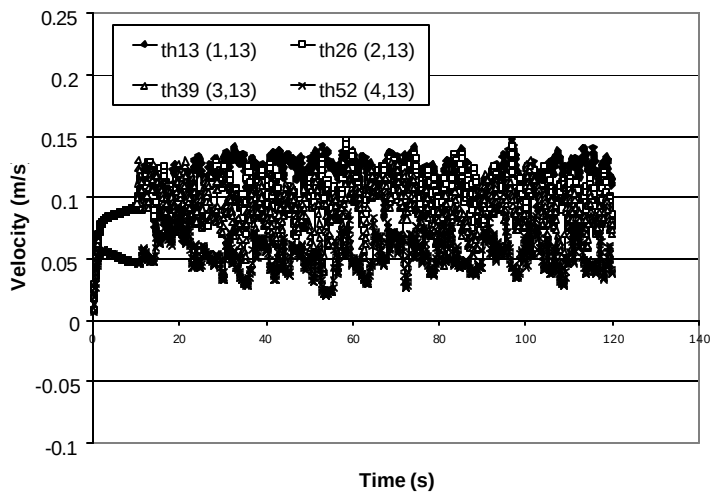

Figure 14 – Time evolution of the velocity for Re=600 measured at x=0.914 m

5. Conclusions

A systematic evaluation of the stability of a re-circulation zone behind a backward facing step has been conducted. The parameters studied have been the flow velocity, step height, and temperature. Numerical modeling using LES-3D has been contrasted with the cold flow experimental results. It can be concluded that:

- The re-circulation zone is stable but not stationary for all conditions studied.
- Fluctuations occur, and the amplitude is comparable to the step-height. Amplitude and frequency are functions of the velocity and step height.
- Buoyancy has only a minor de-stabilizing effect. Flow temperatures were increased up to 600°C. This increasing the dimensions of the re-circulation zone, without de-stabilizing the flow.
- Comparison between the numerical and experimental results shows good qualitative agreement. The code tends to over-predict the size of the re-circulation zone.
- Numerically simulations showed that the entry profile has a significant effect on the length and characteristics of the re-circulation zone.

- Three different regimes have been established. For low oxidizer and fuel velocity the flame is established inside the re-circulation zone and resembles a premixed flame.
- As the velocities increase the flame undergoes a transitional regime and finally establishes itself at the boundary between the main flow and the re-circulation flow.In this third regime the flame is anchored at the edge of the step.
- Air entrainment seems to determine these three different regimes.
- The worst case scenario for suppression seems to correspond to the regime where the flame is attached to the leading edge and established in the mixing layer between the re-circulation zone and the main flow.
- Re-ignition is controlled by cooling and mass transport towards the hot plate. A "worst case scenario" for re-ignition is given by maximizing the fuel mass transfer while keeping the characteristic time for cooling of the fuel surface shorter than the characteristic time to attain a flammable mixture.
- The worst case scenario is characterized by a minimum re-ignition time.

6. References

1. The 1987 Montreal Protocol on Substances that Deplete the Ozone Layer, as adjusted and amended by the Second Meeting of the Parties (London, June, '90) and by the 4th Meeting of the Parties (Copenhagen, Nov., '92) and further adjusted by the 7th Meeting of the Parties (Vienna, Dec., '95).
2. Hamins, A. "Aspects of Flame Suppression," NIST-IR-5766, 1995.
3. Yang, J.C. and Grosshandler, W.L., "Solid propellant Gas Generators: Proceedings of the 1995 Workshop," 1995.
4. Williams, F.A., *"Combustion Theory,"* The Benjamin/Cummings Publ. Company, Inc., 2nd Ed., 1985.
5. Williams, F.A., *Applied Mechanics Surveys*, Abramson, H.N., Liebowitz, H., Crowley, J.M. and Juhasz, S. (Eds.), Washington D.C., Spartan Books, 86-91, 1966.
6. Blazowski, W.S., *Progress in Energy and Combustion Science*, **4**, 177, 1978.
7. Fendell, F.A., *Journal of Fluid Mechanics*, **21**, 281-303, 1965.
8. Fendell, F.A., *Chemical Engineering Science*, **22**, 1829-1837, 1967.
9. Ingason, H. and deRis, J., "Flame Heat Transfer in Storage Geometries," Department of Fire Safety Engineering Report, LUTVDG/TVBB-1013, Lund University, Sweden, 1996.
10. Munson, B.R., Young, D.F. and Okiishi, T.H., "Fundamentals of Fluid Mechanics," Third Edition, John Wiley & Sons, Inc., pp.577, 1998.
11. Armaly, B.F., Durst, F., Pereira, J.C.F., Stoning, B. "Experimental and theoretical investigation of backward-facing step flow**,"** J. Fluid Mech., **127**, pp.473-496, 1983.
12. Sinha, S.N., Gupta, A. K., Oberai, M.M., "Laminar separating flow over backsteps and cavities, Part I: Cavities**,"** AIAA J., **19**, pp.1527-1530, 1981.
13. Denham, M.K., Patrick, M.A., "Laminar flow over a down-stream facing step in a two-dimensional flow channel**,"** Trans. Inst. Chem. Engrs. **52**, pp.361-367, 1974.
14. Takahashi, F., Schmoll, W.J., Strader, E.A. and Belovich, V.M., "Suppression of a Nonpremixed Flame Stabilized by a Backward Facing Step," *Combustion and Flame*, **122**, pp.105-116, 2000.
15. Kanury, M., "Ignition of Liquid Fuels", *The SFPE Handbook of Fire Protection Engineering*, 2nd Edition, NFPA, Quincy, 1995
16. Niioka, T., "Ignition time in the stretched-flow field", Eighteenth Symp. (Intl) on Combustion, 1981
17. Fernadez-Pello, Carlos, "The Solid Phase", *Combustion Fundamentals of Fire*, Academic Press Ltd.,1995
18. McGrattan, K.B., Baum, H.R. and Rehm, R.G. "Large Eddie Simulation of Fire Phenomena," NIST Internal Report, Gaithersburg, Maryland, 1997.
19. DuBois, J., "Evaluation of a Large Eddy Simulation's Applicability to a "Worst Case" Fire Scenario" MS Thesis, University of California, Berkeley, California, December 1999.